Clays and Clay Minerals, Vol. 68, No. 3:250–261, 2020

PURIFICATION OF TURKISH BENTONITES AND INVESTIGATION OF THE CONTACT ANGLE, SURFACE FREE ENERGY AND ZETA POTENTIAL PROFILES OF ORGANO-BENTONITES AS A FUNCTION OF CTAB CONCENTRATION

H. Çiftçi[1]*, B. Ersoy[1], and A. Evcin[2]

[1]Mining Engineering Department, Afyon Kocatepe University, Afyonkarahisar, Turkey
[2]Material Sciences and Engineering Department, Afyon Kocatepe University, Afyonkarahisar, Turkey

Abstract—Purification of raw bentonites and organo-bentonite preparations is sometimes required for industrial use. Zeta (electrokinetic) potential (ζ), contact angle (wettability/hydrophobicity), and surface free energy (SFE) are important surface characteristics and vary significantly according to the applied surfactant concentration when preparing organo-bentonite. Changes in these characteristics determine the stability, behavior, and efficiency of organo-bentonites in various applications such as adsorption, composite materials, and drug-delivery systems. Knowing how much surfactant should be used to prepare organo-bentonite is, therefore, critical. The purpose of the present study was to determine the effect of concentration of the cationic surfactant cetyltrimethylammonium bromide (CTAB) adsorbed in organo-bentonite (prepared from two local and commercial raw bentonites with potential for use in adsorbent and composite materials) on the ζ potential, contact angle, and SFE profiles. The raw bentonites were purified using sedimentation and centrifugation techniques prior to preparation of the organo-bentonite. The purification results were evaluated in light of X-ray diffraction (XRD), cation exchange capacity (CEC), free swelling volume (FSV), X-ray fluorescence (XRF), and particle-size analysis data. Most of the gangue minerals (feldspar, calcite, clinoptilolite, opal, quartz, and mica) having particle size >5 μm were removed from the raw bentonites by using a one-stage sedimentation or a Falcon gravity separator (FGS). Higher yields (68.8% and 81.3% for two bentonites) were obtained with the FGS compared to sedimentation while purification levels were almost the same. ζ changed greatly from –35 mV (and –40 mV) toward 38 mV (and 40 mV) with increasing CTAB concentrations. Similar profiles were also obtained for wettability; maximum contact angles for organo-bentonites were measured as ~72–73°, while they were 12.65 and 14.1° for two purified and unmodified bentonites. SFEs were calculated using contact-angle data, and decreased to minimum values of 41.5–43.6 mJ/m^2 from 78.6–78.2 mJ/m^2 upon treatment of raw bentonites with CTAB. 100–130% CEC concentration was sufficient to prepare organo-bentonites with maximum hydrophobicity and positively charged surfaces.

Keywords—Bentonite · Contact angle · Montmorillonite · Organo-bentonite · Purification · Surface free energy · Zeta potential

INTRODUCTION

Bentonite, consisting predominantly of smectite minerals (montmorillonite, saponite, nontronite, etc.) with a layered structure, is a hydrous aluminum and magnesium silicate with a particle size of <2 μm (Lagaly and Dekany 2013). Bentonite is used for many purposes because of its outstanding characteristics such as large surface area, high CEC, plasticity, swelling ability, biocompatibility, muco-adhesiveness, good mechanical properties, and chemical stability (Yıldız and Kuşcu 2007; Nones et al. 2015; Chenliang et al. 2017). Bentonites are generally used as drilling muds, adsorbents in separation processes, drug-delivery systems, catalysis, composite materials, lubricants in emulsions, food additives for prevention of aflatoxicosis, anti-bacterial material in dental infection, and food-packaging materials, and as a raw material in the cement, ceramics, and pharmaceutical industries (Falaras et al. 1999; Carraro et al. 2014; Yang et al. 2016; Jayrajsinh et al. 2017). Raw bentonites generally contain gangue (non-clay) minerals such as quartz, opal, calcite, feldspar, zeolite, and illite. Some bentonites containing high levels of gangue minerals are classified as low-quality bentonites (Gong et al. 2016). In some applications, such as pharmaceuticals, cosmetics, food, and nanocomposite materials, low-quality bentonites must be purified before use. Purification methods for bentonites reported in the literature have included sedimentation-centrifugation, ion exchange reaction (Shah et al. 2013), modification-centrifugation (Yeşilyurt et al. 2014), multistage hydrocyclone (Boylu et al. 2010), and chemical decomposition (Veiskarami et al. 2016). A washing process is required when the bentonites are purified by chemical purification methods, particularly for use in sensitive applications such as pharmaceuticals, food, and cosmetics. In addition, solid-liquid separation treatments (filtration, evaporation, or centrifugation) are also required which are either difficult and/or costly processes. Simpler physical methods are needed, therefore, to reduce the cost and to provide cleaner production of pure bentonite. The yield of a purification process is another important issue, and needs to be as high as possible. Purification yields have not been reported in most previous studies, however.

Industrially mined bentonites are rich in expandable clay minerals of the smectite group with negatively charged surfaces resulting in hydrophilic properties (Bergaya et al. 2006; Moslemizadeh et al. 2016). These characteristics mean that they resist the adsorption of anionic, neutral, or hydrophobic

* E-mail address of corresponding author: hakanciftci86@gmail.com
DOI: 10.1007/s42860-020-00070-0

species (Ersoy and Çelik 2004). Bentonites are generally modified with cationic surfactants to eliminate these problems, and the products prepared are called organo-bentonites (Zhou 2011). Quaternary alkylammonium salts such as CTAB are commonly used as cationic surfactants to prepare organo-bentonite. Organo-bentonites are widely investigated as adsorbents (Fatimah and Huda 2013), fillers in polymer nanocomposites with improved mechanical properties (Bergaya et al. 2011), and rheology-control agents in drilling fluids, paints, and cosmetics (Yu et al. 2014; Liang et al. 2015).

Wettability (or hydrophobicity) and ζ potential are two important material characteristics used in surface-modification studies. They are encountered in many areas such as mining, textile, paper, medicine, plastic, paint, and food processing (Erol et al. 2017). Wettability is measured by the contact angle between a solid surface and a drop of water. The greater the contact angle, the lower the degree of wettability. For example, a solid having a contact angle of 90° is defined as hydrophobic (non-wettable), and super hydrophobic if >150°. Materials are called hydrophilic (wettable) if the contact angle is close to zero. ζ potential is the measurable electrical charge on the surface of a particle in a liquid. The strength of the electrostatic repulsive forces between the particles and, therefore, the stability of a colloidal system are determined by ζ (Çelik 2004). In addition, the adsorption capacity of a particle is heavily dependent on ζ potential.

Wettability and ζ potential are also important surface characteristics of organo-clays. Determination of the relationship between applied amounts of cationic surfactant and surface characteristics of organo-clays is necessary for some applications. In the literature, similar studies dealing with the preparation of organo-bentonites using alkylammonium salts are reported; a search of the literature revealed that wettability (contact angle) of organo-bentonites depending on the amount of CTAB was investigated in only two studies, however (Zhang et al. 2014; Schampera et al. 2016), and SFE in only one study (Zhang et al. 2014). On the other hand, several studies have determined ζ profiles of organo-bentonites. Zhang et al. (2014) reported the neutralization point of CTAB-modified bentonite at 0.6 mmol/g (49.6% CEC) while the maximum ζ potential (~41 mV) was determined at 1.5 mmol/g (123% CEC) concentration. Barany et al. (2015) showed that the surface of organo-bentonite was neutralized when CTAB concentration reached ~2 mmol/g, and the maximum ζ was determined as 35–40 mV at 7 mmol/g CTAB concentration. Bianchi et al. (2013) prepared organo-montmorillonite samples with three different CTAB concentrations, and maximum ζ was reported as ~35 mV at 100% CEC (1.74 mmol/g) in the pH range of 6.5–7.0. A remarkable decrease in ζ potential (up to 5 mV) at 200% CEC (3.48 mmol/g) concentration was also reported. Such varied or surprising results for the maximum ζ and neutralization points may be due to the use of different CEC values for of the bentonites, different methods of organo-bentonite preparation, and perhaps improper measurements obtained by the use of non-calibrated instruments. The CEC of bentonite is not taken into account when determining the CTAB concentration in most studies.

The objectives of the present study were: (1) to improve the purification of raw bentonites using simple physical methods (sedimentation and centrifugation) in order to obtain high yields; and (2) to investigate the effect of CTAB concentration in organo-bentonite on their wettability (contact angle), ζ potential, and SFE profiles, taking into account the CEC of the bentonite.

MATERIALS AND METHODS

Materials

Two commercial, raw Na-bentonites were investigated in the present study. The first one (labeled as Bent-A) was collected from the mine site of Samaş Industrial Mines Company located in Reşadiye-Tokat, Turkey, and the second one (Bent-B) was collected from a mine site of Çanbensan Industry and Trade Co. Ltd. located in Kalecik-Ankara, Turkey. The manufacturers are market leaders in Turkey and these bentonites have been investigated in many studies (Boylu et al. 2012; Yeşilyurt et al. 2014), including in the preparation and characterization of organo-bentonites (Yeşilyurt et al. 2014; Hojiyev et al. 2016), preparation of clay-polymer nanocomposites (Hojiyev et al. 2017), and adsorption behavior (Orucoglu and Haciyakupoglu 2015). Diiodomethane (CH_2I_2; 99%), used for SFE measurements, and ethanol (C_2H_5OH; 96%) were purchased from Merck (Boston, Massachusetts, USA), and CTAB ($C_{19}H_{42}BrN$; 95%) was purchased from Sigma-Aldrich (St. Louis, Missouri, USA).

Purification of Raw Bentonites

Raw bentonite aggregates were crushed to <5 mm particle size by using a laboratory-scale roller mill crusher. Na-bentonite is easily dispersed in water, and, therefore, no further size reduction was applied in order to avoid reduction of the particle size of gangue minerals. Clay dispersion was prepared in a 2000 mL beaker using 1980 mL of distilled water and 20 g of crushed bentonite sample. The prepared dispersion was allowed to stand for 24 h to ensure the swelling and dispersion of the clay minerals as much as possible (Fig. 1a). Subsequently, the dispersion was stirred mechanically for 30 min at 1000 rpm, and left to sediment for 8 h to allow gangue minerals to settle. The settling behavior of particles in a dispersing system is described by Stokes' law. The necessary settling time (8 h) of gangue minerals having particle sizes >2 μm was calculated according to Stokes' equation. Finally, the suspended dispersion was decanted at the end of the settling time and stored in a beaker. The dispersions obtained were labeled as "Bent-A-Sed" and "Bent-B-Sed" for Bent-A and Bent-B, respectively. Decantation was continued to a height of 3 cm from the bottom of the beaker to prevent the mixing of the settled minerals to the suspended dispersion as a result of turbulence (Fig. 1a).

FGS with small modifications was used as another purification method. Experiments were carried out at 300×*g* centrifugal force and 1.5 L/min feed rate. Fluidizing water was not

https://doi.org/10.1007/s42860-020-00070-0 Published online by Cambridge University Press

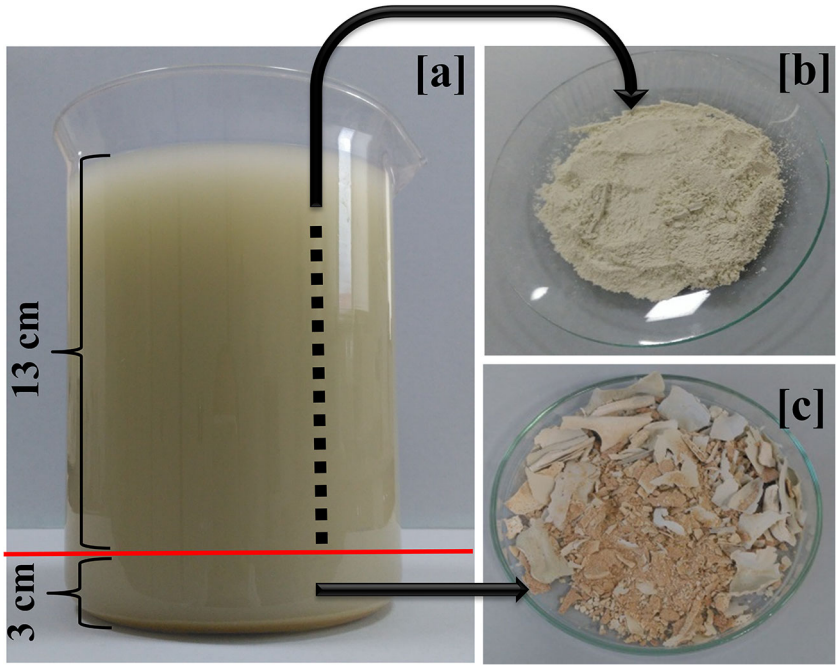

Fig. 1 Photographs of **a** the Ben-A-Raw dispersion, **b** Bent-A-Sed, and **c** gangue minerals.

used, and the water holes in the concentrator bowl were sealed with tape during the experiments. First, the clay dispersion was prepared as in the sedimentation procedure, and then left to stand for 10 min to allow the coarse particles to settle. Subsequently, the dispersion remaining on the settled particles was decanted completely and fed once to the FGS. The products obtained from Bent-A and Bent-B in this step were labeled as "Bent-A-FGS" and "Bent-B-FGS", respectively.

Surface Modification of Purified Bentonites (Organo-bentonite Preparation)

Organo-bentonites were prepared from Bent-A-Sed and Bent-B-Sed samples. The concentrations of CTAB were prepared by adding amounts equal to various fractions of the CEC of the purified bentonites (Bent-A: 95 meq/100 g and Bent-B: 90 meq/100 g) and ranged from 50 to 200% of CEC. As an example, for Bent-A, 100% CEC indicates that 95 mmol CTAB was added for each 100 g Bent-A purified by sedimentation. In the first step, all samples were dried for 24 h at 80°C, ground using a ring mill, and then 5 g of sample was dispersed mechanically in 500 mL of distilled water. Meanwhile, the amount of CTAB required was dissolved in 50 mL of ethanol with magnetic stirring for 30 min and the solution obtained was added dropwise to the clay dispersion. The final mixture was stirred mechanically at 750 rpm for 90 min to ensure that the adsorption and intercalation of cetyltrimethylammonium (CTA^+) ions were completed. Finally, the organo-bentonite obtained was filtered, washed several times with distilled water to remove excessive ions, and then dried for 24 h at 80°C. Products obtained from Bent-A-Sed and Bent-B-Sed were labeled as Organo-Bent-A and Organo-Bent-B, respectively.

Characterization Techniques

Mineralogy and morphology. Mineralogical analysis was performed using a Shimadzu XRD-6000 instrument with CuKα radiation (λ: 1.54184 Å) at 40 kV. The samples were scanned over the angular range 2–70°2θ with a scan rate of 0.02°2θ/step. The raw and purified samples were analyzed after drying under normal atmospheric conditions. The clay mineralogy was also determined for oriented samples and, for these three samples, were prepared for both bentonite samples. Firstly, dispersions containing clay particles were obtained from raw samples by 15 min of sedimentation at a 1.0 wt.% solid:liquid ratio. A few drops of dispersion were then dropped onto the glass slides and allowed to air dry overnight. One of the dried samples was saturated with ethylene glycol vapor at 60°C, while one was heated at 550°C for 2 h. Subsequently, XRD analyses were performed on air-dried, ethylene glycol-saturated, and heated samples (Brown and Brindley 1980). A Jeol 2100F transmission electron microscope (TEM) and LEO 1430 VP scanning electron microscope (SEM) were used to examine the morphology of the bentonite samples.

Chemical and thermogravimetric analyses. The chemical compositions of the samples were determined using a Rigaku ZSX Primus II XRF spectrophotometer. The temperature-related reactions and mass losses were recorded by DTA-TG analysis. For this purpose, Netzsch's differential scanning calorimeter was used and the analysis were carried out from room temperature to 1000°C in argon gas flow with a heating rate of 10°C/min.

https://doi.org/10.1007/s42860-020-00070-0 Published online by Cambridge University Press

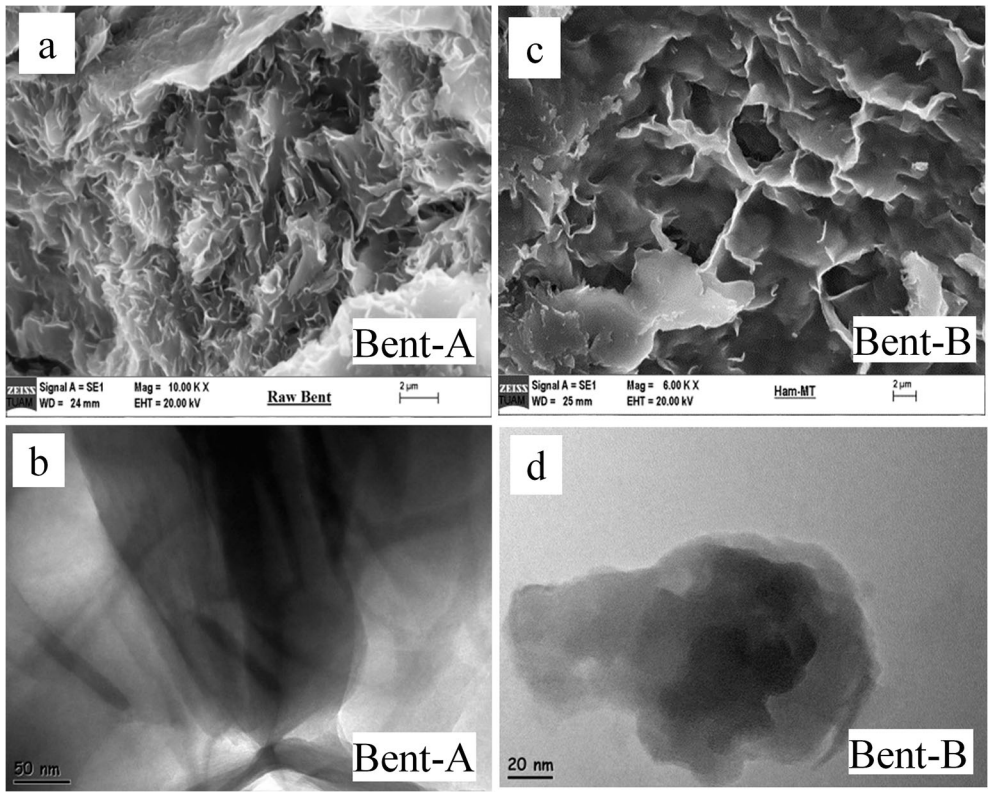

Fig. 2 **a**, **c** SEM and **b**, **d** TEM images of the bentonites.

Determination of cation exchange capacity (CEC) and free swelling volume (FSV). CEC is the number of equivalents of exchangeable cations between the clay mineral layers per 100 g of clay. The CECs of bentonites were determined by the methylene blue (MB) test according to the ASTM D 5890-95.

Standard and the procedure can be summarized as follows. A 2 g of sample was dried for 24 h at 105°C and then ground using a ring mill. The sample was then added to a 600 mL beaker containing 300 mL of distilled water and the dispersion was stirred using a magnetic stirrer until complete dispersion. The pH of the prepared dispersion was adjusted to between 2.5 and 3.8 using 2 N H_2SO_4 solution. Stirring was then continued for 10–15 min and the pH was adjusted again if necessary. While stirring was continued, 5 mL of 10^{-2} M MB solution (1 mL = 0.01 meq) was added to the dispersion and stirring continued for 1–2 min. One drop of suspension was then taken using a glass rod and left on the filter paper (Sartorius 392). The last two steps were continued until formation of a light blue halo around the drop. When the halo appeared, a drop was taken from the dispersion after 2 min without adding MB, and left on the filter paper. The end point was reached if the halo was formed. If the halo was not observed, further 1-mL aliquots of MB solution were added to the dispersion until the end point was reached. The CEC was calculated using Eq. 1.

$$CEC = \frac{EV}{W} \times 100 \quad (1)$$

where *CEC* is cation exchange capacity (meq/100 g), *E* is the miliequivalent value for 1 mL of MB, *V* is the amount of methylene blue (mL) used in titration, and *W* is the amount of clay (g).

The MB test is used commonly for determination of the CEC of clays; some limitations have been reported for this method, however. Possible dye–dye interactions can increase the bilayer adsorption of dye cations on the surface of clay minerals. In addition, aggregation of dye molecules can occur on the external surfaces (Lagaly et al. 2013). The method is used widely because of its simple and fast application. In the bentonite industry, smectite contents (product qualities) are often quantified using MB adsorption; comparability is usually based on MB adsorption of a reference material with known smectite content, however. This requires assumption of a similar layer-charge density. Additionally, diluted MB solution should be added gradually to the clay/water dispersion as described above. Otherwise, clay surfaces are quickly covered by large MB molecules and clay aggregates are formed. This prevents the intercalation of the MB molecules (Taylor 1985; Rytwo et al. 1991; Kahr and Madsen 1995).

FSV is caused by hydration of interlayer surfaces of the clay mineral, resulting in a larger total volume due to the penetration of water molecules between the layers. FSV measurements were performed according to ASTM 837 C standard. A ground sample with a particle size of <150 µm was dried at 105°C for 24 h. 90 mL of distilled water was added to a 100 mL graduated cylinder. Approximately 0.1 g of clay was added slowly to the

https://doi.org/10.1007/s42860-020-00070-0 Published online by Cambridge University Press

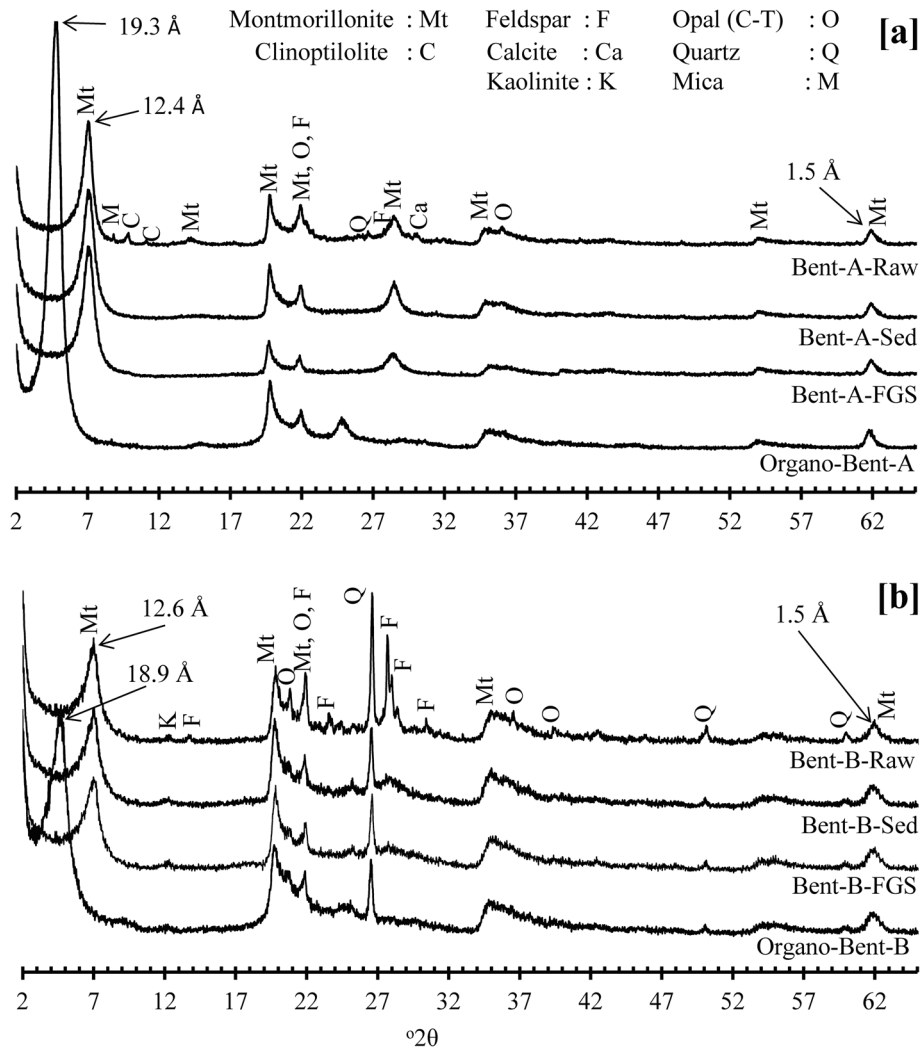

Fig. 3 XRD patterns of the raw, purified, and organo-bentonites: **a** Bent-A, and **b** Bent-B.

cylinder each time. The added clay was allowed to settle for a minimum period of 10 min. The two previous steps were repeated until 2 g of dried clay sample had been added to the cylinder. Mineral particles adhering to the cylinder edges were then dispersed into the water by adding more water until the level reached 100 mL. After that, the dispersion was allowed to stand for 16 h. Finally, the volume of hydrated clay mass standing at the bottom of the cylinder was recorded by reading from the graduated scale on the cylinder.

Surface properties and particle size-distributions. The wettability of the Bent-A-Sed and Bent-B-Sed samples loaded with various concentrations of CTAB was determined by contact-angle measurements. First, 2×25 mm discs were prepared from dried and ground powders under 50 kN pressure using a manual hydraulic press (Specac Co., London, UK). Then, 5 μL of distilled water (a drop) was placed on each disc-shaped sample using a Hamilton injector. The contact angles were then measured with a One Attension theta optical goniometer (Biolin Scientific Co., Espoo, Finland) using the sessile drop method at room temperature. The value obtained at the fifth second immediately after dropping the water drop on the sample surface was recorded as the contact angle. At least three measurements were performed for each sample and the averages of the results recorded. Contact angles of each sample were also measured using diiodiomethane to calculate SFE according to the OWRK/Fowkes method (Fowkes 1962; Owens and Wendt 1969; Kaelble 1970). Once the contact angles for water and diiodiomethane were determined, the SFE calculations were performed automatically by the instrument.

Measurements of ζ were obtained using a Malvern Nano-Z zeta-sizer instrument (Malvern Panalytical Co., Malvern, UK) at room temperature. Dried and ground samples were added to 10^{-3} M NaCl solutions at 0.01 wt.% solid:liquid ratio, and dispersed for 30 min using a magnetic stirrer. Subsequently, stirring was stopped and the dispersion was left for 5 min to allow coarse particles to settle. One-mL aliquots

https://doi.org/10.1007/s42860-020-00070-0 Published online by Cambridge University Press

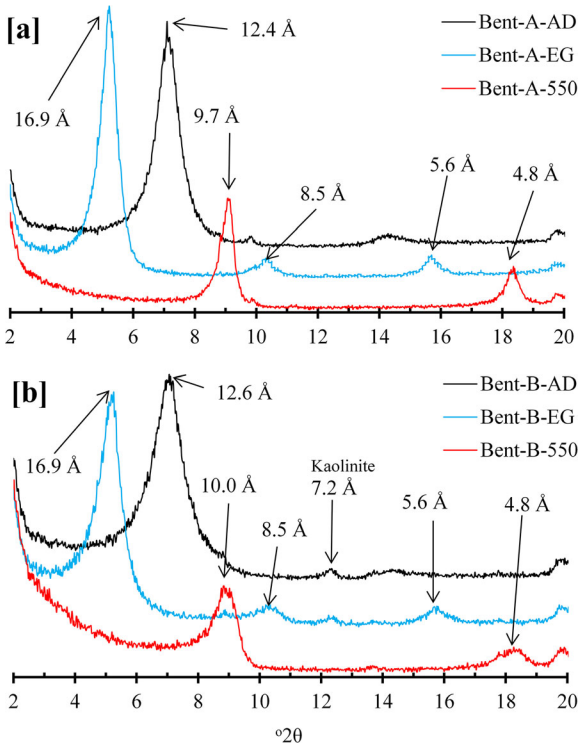

Fig. 4 XRD patterns based on oriented mounts of the bentonites: **a** Bent-A, **b** Bent-B. AD: air dried, EG: ethylene glycol-treated, and 550: heated at 550°C.

were then taken from the dispersions and placed in the measuring cell. ζ values were calculated automatically by the instrument software using the classical Smoluchowski formula and the measured electrophoretic mobility values of particles. The measurements were repeated three times and the results having minimum standard deviations (3–5%) were recorded as ζ values.

Particle-size distributions were determined using a Malvern Mastersizer 2000 instrument (Malvern Panalytical Co., Malvern, UK). Dispersions obtained from sedimentation and FGS were used for analysis. Firstly, a 1000 mL beaker containing 800 mL of distilled water was placed in the pump section of the wet analysis apparatus, stirring was started at 2000 rpm, and then the background was measured. Subsequently, an appropriate amount of each sample was homogenized for 1 min at 400 Watt using a Hielscher UP400S sonicator (Hielscher Ultrasound Technology Co., Teltow, Germany) and added slowly to the beaker until the laser obscuration reached 3–6%. Finally, measurements were started and the average values were recorded by repeating each analysis three times.

RESULTS AND DISCUSSION

Characterization of Purified Bentonites

Smectites (montmorillonite, nontronite, saponite, etc.) usually exhibit a morphology that resembles honeycomb, cornflake, leafy, and rosette-like appearance (Keller et al. 1986). SEM images (Fig. 2a, c) revealed that the bentonite samples consisted of grain aggregates with smooth surfaces, and have leaf-layer morphology with its curved edges. Transmision election microscopy images (Fig. 2b, d) showed that the samples have a multi-layered structure consisting of successive sheets with parallel and flat surfaces.

The XRD patterns of the raw bentonites (Fig. 3) revealed that the samples consisted of smectites, traces of kaolinite (in Bent-B), and gangue minerals such as feldspar, calcite, quartz, opal (C-T), clinoptilolite (zeolite), and mica. Bent-A samples other than organo-bentonites showed characteristic reflections (7.07°2θ) with the d_{001} basal spacing of 12.4 Å confirming Na^+-rich smectites (Brown and Brindley 1980; Hayakawa et al. 2016). Bent-B showed a similar but broader reflection (7.01°2θ) with a d_{001} basal spacing of 12.6 Å (Fig. 3b). Additionally, gangue mineral (especially feldspar) contents were greater in Bent-B when considering the reflection intensities. The d_{060} values (1.5 Å) of the smectites showed that both bentonites were composed of dioctahedral smectites (montmorillonite, nontronite, beidellite) (Grim 1968). Almost all of the gangue minerals were removed from the Bent-A-Raw by sedimentation and FGS. The result for Bent-B was slightly different, and small amounts of quartz and kaolinite remained in both Bent-B-Sed and Bent-B-FGS products as a result of the suspended particles having particle sizes <2 μm. Of course, such small particles may have also remained in the Bent-A-Sed and Bent-A-FGS products, but in very small amounts below the detection limit of XRD. Considering the purification levels, XRD data showed no significant difference between the sedimentation and FGS techniques for both bentonites. The XRD patterns of the oriented mounts of the two bentonites (Fig. 4) revealed that the d_{001} basal spacing of both smectites expanded to 16.9 Å after ethylene glycol (EG) treatment. On the other hand, it collapsed to 9.7 Å for Bent-A and 10.0 Å for Bent-B after heating at 550°C. The differences in basal spacings after heating can be attributed to the exchangeable cation diversity between the smectite layers. The XRD results obtained from oriented samples proved that both samples are dominated by smectite minerals. The change in the basal spacings of smectites of oriented samples is based mainly on the type of the exchangeable cations and magnitude and localization of the layer charge (Harward and Brindley 1965). No chemical pretreatment was performed other than dispersion in deionized water. Basal reflections of air-dried samples at 12.4–12.6 Å indicate the dominance of Na^+ over other exchangeable cat-

Table 1 CEC and FSV values of the raw and purified bentonites.

Sample	CEC (meq/100 g)	FSV (mL/g)
Bent-A-Raw	80.0	25
Bent-A-FGS	92.5	27
Bent-A-Sed	95.0	27
Bent-B-Raw	60.0	9
Bent-B-FGS	87.5	11
Bent-B-Sed	90.0	11

https://doi.org/10.1007/s42860-020-00070-0 Published online by Cambridge University Press

Table 2 Chemical analysis (XRF) data of the raw and purified bentonites.

Component	Content (wt.%)					
	Bent-A-Raw	Bent-A-Sed	Bent-A-FGS	Bent-B-Raw	Bent-B-Sed	Bent-B-FGS
SiO_2	62.23	62.19	61.18	60.32	60.63	60.45
Al_2O_3	19.06	20.2	20.17	17.7	17.61	17.58
Fe_2O_3	3.63	3.99	4.16	5.77	7.21	7.35
MgO	2.7	2.93	2.83	2.89	2.69	2.54
Na_2O	2.61	2.02	2.13	2.46	1.03	1.23
CaO	2.05	0.74	0.61	1.78	1.04	1.15
K_2O	0.65	0.44	0.47	1.30	1.14	1.21
LOI	6.30	7.0	7.50	5.87	7.18	6.92

LOI: loss on ignition

ions. The broader peak of Bent-B (Fig. 4b) indicates the presence of significant amounts of bivalent Ca^{2+}. Additionally, both EG-treated samples showed d_{002} and d_{003} values of 8.5 Å and 5.6 Å, which confirmed that the smectites do not contain significant amounts of interstratified minerals (compare e.g. Kaufhold et al. 2019)

The CEC and FSV data of the raw and purified bentonites (Table 1) revealed that Bent-B-Raw has smaller CEC and FSV values than Bent-A-Raw, indicating greater gangue-mineral contents in the Bent-B-Raw sample. After purification treatments, the CECs of both samples reached similar values. A significant difference was observed between the FSVs of the samples even after purification treatments, and Bent-A samples presented quite large FSVs when compared to Bent-B. This can be explained by the smaller Na^+ content of Bent-B-Sed (Na_2O = 1.03 wt.%; Table 2) compared to Bent-A-Sed (Na_2O = 2.02 wt.%; Table 2) indicating a much larger exchangeable Na content of smectite in Bent-A. This is confirmed by a larger CaO content of Bent-B-Sed (1.04 wt.%; Table 2) compared to Bent-A-Sed (0.74 wt.%; Table 2). CEC and FSV data agreed well with the XRD results, and also successful purification of the raw bentonites.

The XRF analysis data (Table 2) showed that the samples had large percentages of silicon and aluminum oxides (≥80 wt.%), indicating the presence of a clay mineral. (Na_2O+K_2O)/(CaO+MgO) ratios were determined to be 0.67 and 0.58 for

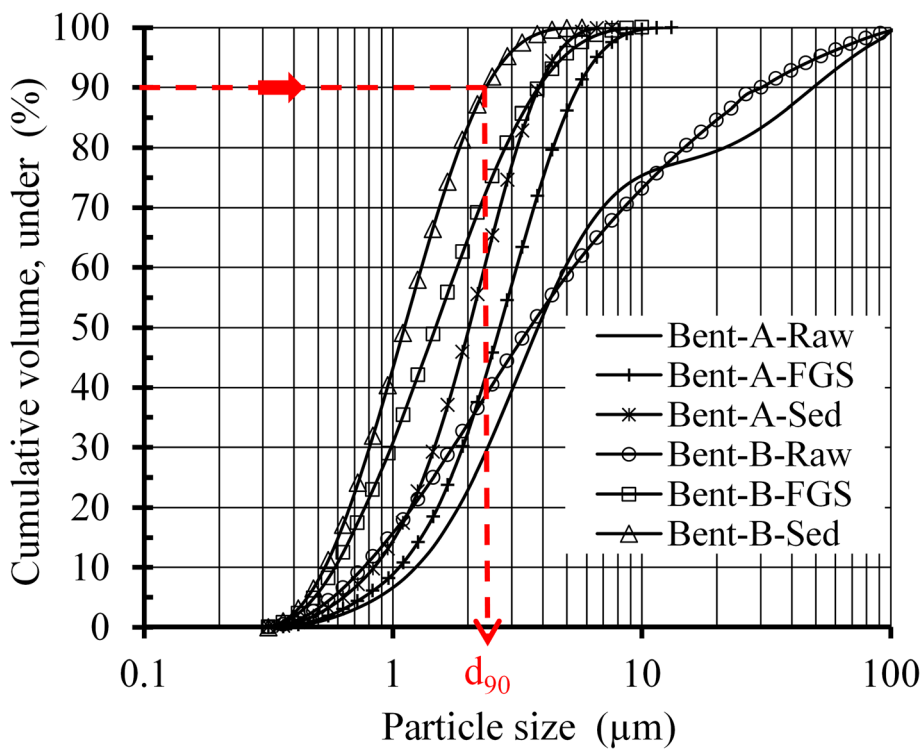

Fig. 5 Particle-size distributions of the raw and purified bentonites.

https://doi.org/10.1007/s42860-020-00070-0 Published online by Cambridge University Press

Table 3 Yields of the purified bentonite products according to separation techniques.

Product	Yield (wt.%)
Bent-A-Sed	67.5
Bent-A-FGS	81.3
Bent-B-Sed	45.0
Bent-B-FGS	68.8

Bent-A-Sed and Bent-B-Sed, respectively, and values >0.33 can be attributed to Na-smectites. Ca^{2+} content in samples decreased significantly after removal of calcite minerals by purification treatments which are in good accordance with XRD data. Compared with that of the raw bentonite, a strong decrease in Na_2O content after purification can be explained by the removal of Na-rich feldspar (anorthoclase) minerals.

Particle-size distributions (Fig. 5) revealed that raw bentonites contain large particles, >10 μm, which can be attributed to non-clay (gangue) minerals. Particle-size distributions of all purified samples were the range 0.3–10 μm. This distribution comprises predominantly pure clay minerals. Shah et al. (2013) also reported similar results and determined the particle-size distribution of bentonite purified by sedimentation to be between 0.3 and 7.5 μm. The d_{10}, d_{50}, and d_{90} values (Fig. 5 and Table 4) show particle sizes, and 10%, 50% and 90% of the sample amount are smaller than these particle sizes, respectively. For example, d_{90} of Bent-A-Sed means that 90% of the sample consists of particles with a size. The majority of the purified bentonite particles have a particle size <5 μm and puts them close to the clay particle-size range (Lagaly and Dekany 2013). The minimum particle size for all samples was measured to be ~0.3 μm. Sedimentation products have narrower particle-size distributions with little difference when compared to FGS products. The data also showed that the difference between the particle size of clay and non-clay minerals is the main effect on the purification methods used. The particle-size analysis was not performed for organo-bentonites because of agglomeration of particles.

Higher yields for Bent-A and Bent-B (81.3 wt.% and 68.8 wt.%, respectively) were obtained by FGS compared to the sedimentation technique (Table 3), while the purification levels were almost the same for both techniques. Greater gangue-mineral content in the Bent-B sample resulted in lower yield values, which is in accordance with the XRD, CEC, and XRF results.

Table 4 Particle-size distributions of the raw and purified bentonites.

Sample	d_{10} (μm)	d_{50} (μm)	d_{90} (μm)
Bent-A-Raw	1.23	3.82	48.79
Bent-A-Sed	0.84	2.02	3.85
Bent-A-FGS	1.06	2.69	5.34
Bent-B-Raw	0.78	3.54	30.27
Bent-B-Sed	0.53	1.11	2.36
Bent-B-FGS	0.58	1.48	3.84

Characterization of Organo-bentonite

The XRD patterns of organo-bentonites prepared by CTAB concentration of 100% CEC (Fig. 3) showed that the basal spacing expanded to 19.3 Å (2θ: 4.58°) for Bent-A and 18.9 Å (2θ: 4.69°) for Bent-B as a result of the successful intercalation of CTA^+ ions into the interlayer spaces of smectites by the cation exchange process. Similar results for organo-bentonites treated with CTAB at a concentration of 100% CEC were also reported by other research teams (Yılmaz and Yapar 2004; Haloi et al. 2013). Lee and Kim (2002) reported the formation of a bilayer arrangement of CTA^+ ions (17–18 Å) between bentonite layers when loading from 50% to 150% CEC concentration.

The DTA-TG curves of raw, purified, and organo-modified (at 100% CEC concentration) Bent-A samples revealed an intense endothermic reaction in raw bentonite at 150°C (Fig. 6). This is due to removal of adsorbed water on the external and interlayer surfaces of the smectites (Velde 1992). The second endothermic peak observed at 700°C was due to dehydroxylation of the smectite layers. The endothermic peak at 900°C was attributed to phase transformations and degradation of the clay mineral structure (Bulut et al. 2009).

Further analysis of the raw bentonite TG curve (Fig. 6a) found that the first mass loss was ~7–8% between 80 and 170°C, and the second mass loss was ~4% between 625 and 725°C temperature ranges. The Bent-A-Sed sample compared to Bent-A-Raw showed a lower mass loss of ~3% between 80–170°C and this may be due to the small moisture content. The mass loss was approximately the same in the second step, and this may be due to the small amount of gangue minerals (especially calcite) in the sample.

The DTA curve of organo-bentonite showed (Fig. 6c) the first small endothermic peaks at ~90°C and ~150°C which are attributed to the release of free water molecules due to evaporation. The second endothermic peak at ~310°C is related to decomposition of CTA^+ ions and their micelles adsorbed on the surface of the clay (Houhoune et al. 2016). The third peak at ~420°C is attributed to the decomposition of CTA^+ molecules intercalated in the interlayer spaces of the smectites (Majdan et al. 2010). The last two endothermic peaks at ~600°C and ~900°C are associated with dehydroxylation of clay layers and phase transformations of clay minerals, respectively. The TG curve of organo-bentonite (Fig. 6c) showed an additional weight loss (21.7%) between 200°C and 640°C which can be attributed to the degradation of cationic surfactants on the external surfaces and in the interlayer spaces of the smectites.

The ζ profiles of purified bentonites (Fig. 7 and Table 5) revealed that the surface electro kinetics of the bentonites is heavily dependent on CTAB concentration. The 0% CEC points indicate the ζ of the CTAB free purified bentonites, and the measured values (Bent-A-Sed; -38.7 mV and Bent-B-Sed; –35.7 mV) are in good agreement with the literature (Barany et al. 2015; Zhang et al. 2014; Barany et al. 2015). Bent-A and Bent-B displayed similar profiles and the ζ of both moved dramatically towards positive values with increasing

https://doi.org/10.1007/s42860-020-00070-0 Published online by Cambridge University Press

Table 5 Summarized surface characteristics of the samples.

Sample	Neutralization point (% CEC)	Max. ζ		Max. contact angle		Min. SFE	
		CTAB conc. (% CEC)	mV	CTAB conc. (% CEC)	(°)	CTAB conc. (% CEC)	mJ/m^2
Organo-Bent-A	86	140	39.8	110	71.9	100	39.6
Organo-Bent-B	78	120	38.5	80	72.4	100	36.2
	ζ (mV)			Contact angle (°)		SFE (mJ/m^2)	
Bent-A-Sed	–38.7			12.7		66.0	
Bent-B-Sed	–35.7			14.1		67.3	

CTAB concentration. This can be explained by the fact that CTA^+ ions were also adsorbed on clay surfaces as they intercalated into the interlayer spaces. In addition, adsorption of CTA^+ ions on the external surface is easier and faster than intercalation in the early stages of treatment. The surfaces of organo-bentonites were neutralized at concentrations of 78–86% CEC (0.68–0.77 mmol/g). Maximum values of ζ of Bent-A and Bent-B were measured as 39.8 mV and 38.5 mV at 140% CEC (1.23 mmol/g) and 120% CEC (1.08 mmol/g) concentrations, respectively. No significant change in ζ was observed in either bentonite with more than 120% CTA^+ applied. At this applied concentration, monolayer adsorption on the surface was completed, but intercalation continued. In addition, partial bilayer adsorption or micelle formation of the CTA^+ ions could have occurred on the surface. The pH of the dispersions prepared for ζ analysis of raw bentonite and organo-bentonite were 9.6 and 7.1, respectively (Fig. 7). The pH of the distilled water was 5.7. The CTAB concentration did not have a significant effect on pH.

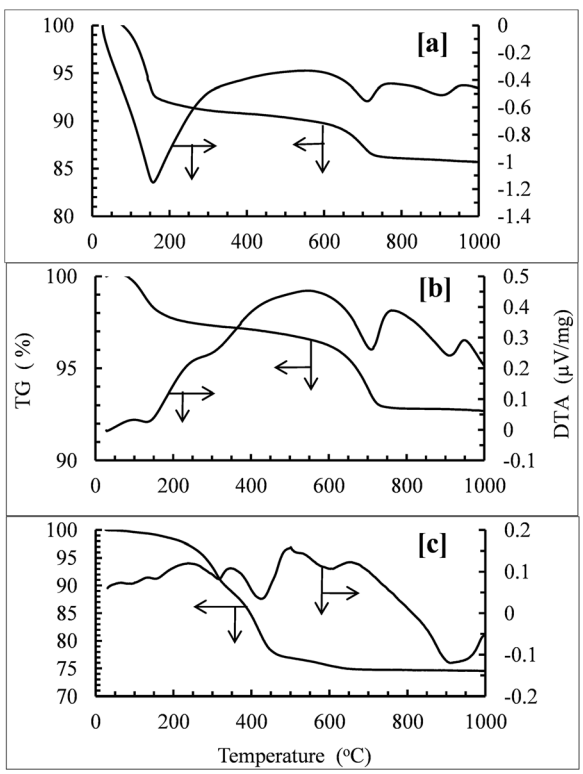

Fig. 6 DTA-TG curves of **a** the Bent-A-Raw, **b** Bent-A-Sed, and **c** Organo-Bent-A.

The wettability of the purified bentonites was investigated by measuring the contact angles with distilled water. Significant changes of the contact angle were observed depending on the CTAB concentration, ranging from super hydrophilic to partial hydrophobic (Fig. 8 and Table 5). This is attributed to the neutralization of Lewis base sites (O atoms on the surface) by adsorption of organic cations (Jai Prakash 2004). The ζ and contact angles initially change rapidly because of the rapid adsorption of the large CTA^+ ions onto the external surfaces; intercalation into the smectites interlayer spaces is initially more difficult until some layer expansion occurs. Intercalation is then easier and takes less time. The 0% CEC point indicates the contact angles of the CTAB free Bent-A-Sed and Bent-B-Sed samples to be 12.7° and 14.1°, respectively. Low contact angles (high hydrophilicty or low hydrophobicity) result from the hydration of exchangeable cations. All clay minerals except the uncharged minerals talc and pyrophyllite exhibit such behavior when they come into contact with liquids (Grim 1968). The maximum contact angle or Bent-A-Sed was measured to be 71.9° at the CTAB concentration of 110% CEC while it was 72.4° at 80% CEC for Bent-B-Sed. Schampera et al. (2016) reported the contact angle of Wyoming bentonite (MX-80) modified by cetyltrimethylammonium chloride (CTACl) as being 105° and 52° at 40% and 200% CEC concentrations, respectively. Zhang et al. (2014) determined the maximum contact angle for organo-bentonite to be 105°. The two teams have also determined the decrease in contact angle after reaching a plateau with further increase in CTAB concentration. Different contact angle values obtained from various studies can be caused by variations in the organo-bentonite preparation and on which contact-angle measuring methods were employed. The increase in contact angle is caused by the hydrophobic character of the hydrocarbon tails which are directed away from the smectite surface as a result of adsorption of the polar heads of CTA^+ ions on the surface. The contact angles of both samples decreased slightly after 100% CEC concentration, which may be explained by the formation of bilayer adsorption or micelles on the external surfaces after the active sites are completely occupied by CTA^+ ions.

https://doi.org/10.1007/s42860-020-00070-0 Published online by Cambridge University Press

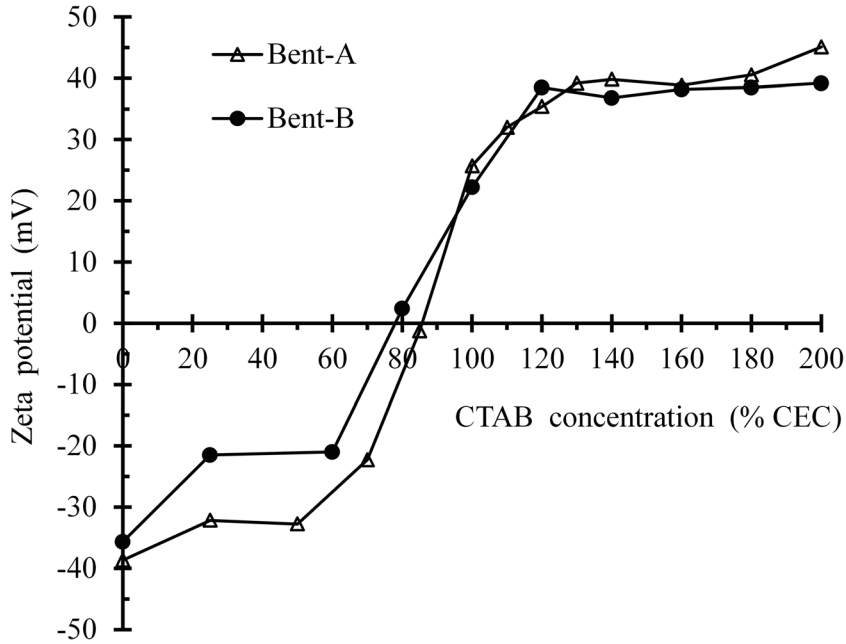

Fig. 7 Zeta potential (ζ) profiles of bentonites loaded with CTA^+ at various concentrations.

The surface free energy (γ_i) of a solid surface (i) is theoretically equal to half of the cohesive energy (ΔG_{ii}) that holds both surfaces together (Jai Prakash 2004). γ_i is the sum of the free energy components of Lifshitz-van der Waals (γ_i^{LW}) and Lewis acid-base (γ_i^{AB}) interactions as shown in Eq. 2 (van Oss et al. 1988). γ_i^{LW} is the surface free energy component emerging with van der Waals (London, Debye, and Keesom) forces resulting from apolar interactions. γ_i^{AB} is a surface free energy component that results from polar interaction forces on the surface capable of receiving electrons (Lewis acid) or electron-donating (Lewis base).

$$\gamma_i = \gamma_i^{LW} + \gamma_i^{AB} \quad (2)$$

Interactions in the solid–liquid interface have not yet been fully expressed mathematically and, therefore, the methods of calculating SFE using the contact angle data have different

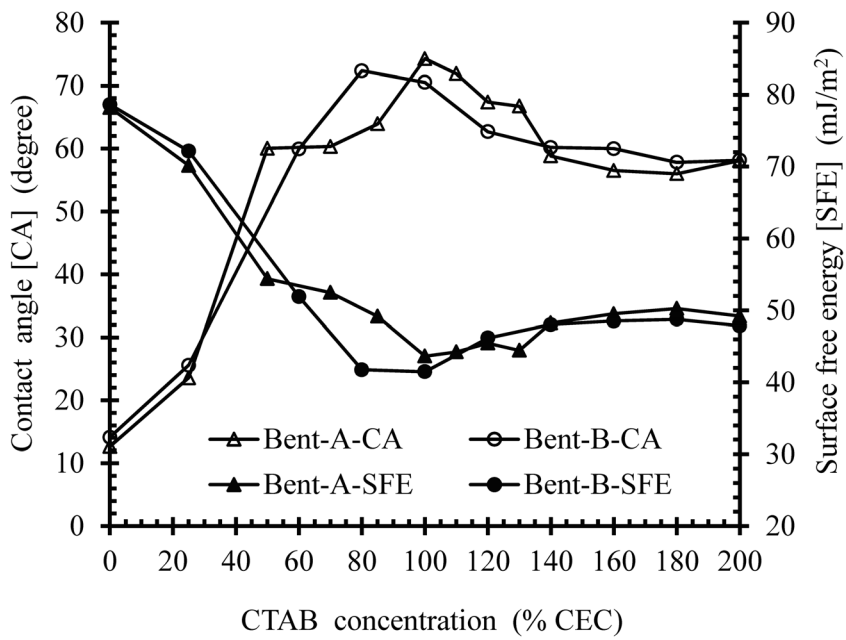

Fig. 8 Contact angle (Bent-A-CA, Bent-B-CA) and surface free energy (Bent-A-SFE, Bent-B-SFE) profiles of bentonites loaded with CTA^+ at various concentrations.

https://doi.org/10.1007/s42860-020-00070-0 Published online by Cambridge University Press

assumptions. As a result, the measured values of the SFE of solids may be different from each other according to the methods used.

In the present study, as expected, the measured SFEs of purified and organo-bentonites exhibited a trend in contrast to the contact angle profiles (Fig. 8). The SFEs of the CTAB-free purified Bent-A and Bent-B were determined to be 78.2 and 78.6 mJ/m^2, respectively. SFEs decreased significantly with CTAB concentration increasing up to 80–100% CEC. The SFEs of both samples were then changed slightly and fixed. Minimum SFEs were calculated to be 43.6 mJ/m^2 for Bent-A and 41.5 mJ/m^2 for Bent-B at 100% CEC concentration. Zhang et al. (2014) also reported a similar SFE profile for organo-bentonites according to the CTAB concentration, giving a minimum SFE of ~35 mJ/m^2. As a result, solids having high SFE, such as bentonite, can be wetted by most liquids, and vice versa. In addition, the stabilization of organo-clays is very limited, while unmodified clays can easily form stable suspensions with water (hydrophilic character).

CONCLUSIONS

The raw bentonites were purified by sedimentation and FGS separation techniques, both of which techniques are based on differences in particle sizes of clay and non-clay minerals. While small amounts of quartz could not be removed from the Bent-B sample, no gangue (non-clay) mineral in purified Bent-A samples was detected by XRD. Separation of the <5 μm gangue minerals from clay minerals was quite difficult for both techniques under the conditions used. Modified FGS would be a better choice for purifying raw bentonites in a much shorter time and at higher yields; separation of <5 μm gangue minerals from clay minerals is not possible using these techniques, however.

X-ray diffraction and surface characterization analyses indicated that CTA^+ ions were adsorbed on external surfaces as well as intercalated into the interlayer spaces of smectites. Zeta potential and contact-angle measurements showed that the electrodynamic and chemical surface properties of clay particles can be altered significantly by adsorption of surfactant molecules on the clay surfaces. Negative surface charges of Na-smectites were converted to positive values up to a certain CTAB concentration. ζ reached a plateau at 39.2 mV (at 130% CEC concentration) and 38.5 mV (at 120% CEC conc.) for Bent-A-Sed and Bent-B-Sed, respectively. No significant change in ζ was then recorded for either bentonite with further increase of CTAB concentrations. Loading of the clay minerals with CTA^+ molecules resulted in the formation of a partially hydrophobic surface with maximum contact angles of ~74.3° (at 100% CEC concentration) and 72.4° (at 80% CEC concentration) for Bent-A-Sed and Bent-B-Sed, respectively. Slight decreases in contact angle were seen at higher concentrations. The CTAB concentration of ~100–130% CEC is, therefore, sufficient to prepare organo-bentonites with maximum hydrophobicity and positively charged surfaces.

ACKNOWLEDGMENTS

This study was supported financially by Afyon Kocatepe University, Scientific Research Project (BAP), Project No: 18.FEN.BIL.06 and 18.KARIYER.107. The authors are grateful to the journal's editors and reviewers.

REFERENCES

Barany, S., Meszaros, R., Taubaeva, R., & Musabekov, K. (2015). Electrosurface properties of kaolin and bentonite particles in solutions of electrolytes and surfactants. *Colloid Journal, 77*, 692–697.

Bergaya, F., Theng, B. K. G., & Lagaly, G. (2006). *Handbook of Clay Science* (1246 pp). Amsterdam: Elsevier.

Bergaya, F., Jaber, M., & Lambert, J. F. (2011). Organophilic clay minerals. In M. Galimberti (Ed.), *Rubber Clay Nanocomposites-Science, Technology and Applications* (pp. 45–86). New York: John Wiley and Sons.

Bianchi, A. E., Fernández, M., Pantanetti, M., Viña, R., Torriani, I., Torres Sánchez, R. M., & Punte, G. (2013). $ODTMA^+$ and $HDTMA^+$ organo-montmorillonites characterization: New insight by WAXS, SAXS and surface charge. *Applied Clay Science, 83–84*, 280–285.

Boylu, B., Çinku, K., Esenli, F., & Çelik, M. S. (2010). The separation efficiency of Na-bentonite by hydrocyclone and characterization of hydrocyclone products. *International Journal of Mineral Processing, 94*, 196–202.

Boylu, F., Hojiyev, R., Ersever, G., Ulcay, Y., & Çelik, M. S. (2012). Production of ultrapure bentonite clays through centrifugation techniques. *Separation Science and Technology, 47*, 842–849.

Brown, G., & Brindley, G. W. (1980). X-ray diffraction procedures for clay mineral identification. In G. W. Brindley & G. Brown (Eds.), *Crystal Structures of Clay Minerals and their X-ray Identification*, *Monograph 5* (pp. 305–360). London: Mineralogical Society.

Bulut, G., Chimeddorj, M., Esenli, F., & Çelik, M. S. (2009). Production of desiccants from Turkish bentonites. *Applied Clay Science, 46*, 141–147.

Carraro, A., De Giacomo, A., Giannossi, M. L., Medici, L., Muscarella, M., Palazzo, L., Quaranta, V., & Tateo, F. (2014). Clay minerals as adsorbents of aflatoxin M1 from contaminated milk and effects on milk quality. *Applied Clay Science, 88*, 92–99.

Çelik, M.S. (2004). Electrokinetic behavior of clay surfaces. Pp. 58–89 in: *Clay Surfaces: Fundementals and Aplications* (F. Wypych and K.G. Satyanarayana, editors). Elsevier, The Netherlands.

Chenliang, P., Fanfei, M., Lingyun, L., & Chen, J. (2017). The adsorption of $CaOH^+$ on (001) basal and (010) edge surface of Na-montmorillonite: a DFT study. *Surface and Interface Analysis, 49*, 267–277.

Erol, I., Devrim, D. N., Ciftci, H., Ersoy, B., & Cigerci, I. H. (2017). Novel functional copolymers based on glycidyl methacrylate: Synthesis, characterization, and polymerization kinetics. *Journal of Macromolacular Science, 54*, 434–445.

Ersoy, B., & Celik, M. S. (2004). Uptake of aniline and nitrobenzene from aqueous solution by organo-zeolite. *Environmental Technology, 25*, 341–348.

Falaras, P., Kovanis, I., Lezou, F., & Seiragakis, G. (1999). Cottonseed oil bleaching by acid activated montmorillonite. *Clay Minerals, 34*, 221–232.

Fatimah, I., & Huda, T. (2013). Preparation of cetyltrimethylammonium intercalated Indonesian montmorillonite for adsorption of toluene. *Applied Clay Science, 74*, 115–120.

Fowkes, F. M. (1962). Determination of interfacial tensions, contact angles, and dispersion forces in surfaces by assuming additivity of intermolecular interactions in surfaces. *Journal of Physical Chemistry, 66*, 382–382.

Gong, Z., Liao, L., Lv, G., & Wang, X. (2016). A simple method for physical purification of bentonite. *Applied Clay Science, 119*, 294–300.

Grim, R. E. (1968). *Clay Mineralogy*. International series in the earth and planetary sciences (596 pp). New York: Mc Graw-Hill Book Co. Inc..

Haloi, S., Goswami, P., & Das, D. K. (2013). Differentiating response of 2,7-dichlorofluorescein intercalated CTAB modified Na-MMT clay matrix towards dopamine and ascorbic acid investigated by

https://doi.org/10.1007/s42860-020-00070-0 Published online by Cambridge University Press

electronic, fluorescence spectroscopy and electrochemistry. *Applied Clay Science, 77–78*, 79–82.
Harward, M. E., & Brindley, G. W. (1965). Swelling properties of synthetic smectites. *Clays and Clay Minerals, 13*, 209–222.
Hayakawa, T., Minase, M., Fujita, K.-I., & Ogawa, M. (2016). Modified method for bentonite purification and characterization; A Case Study Using Bentonite from Tsunagi Mine, Niigata, Japan. *Clays and Clay Minerals, 64*, 275–282.
Hojiyev, R., Ersever, G., Karaağaçlıoğlu, İ. E., Karakaş, F., & Boylu, F. (2016). Changes on montmorillonite characteristics through modification. *Applied Clay Science, 127–128*, 105–110.
Hojiyev, R., Ulcay, Y., & Çelik, M. S. (2017). Development of a clay-polymer compatibility approach for nanocomposite applications. *Applied Clay Science, 146*, 548–556.
Houhoune, F., Nibou, D., Chegrouche, S., & Menacer, S. (2016). Behaviour of modified hexadecyltrimethylammonium bromide bentonite toward uranium species. *Journal of Environmental Chemical Engineering, 4*, 3459–3467.
Jai Prakash, B. S. (2004). Surface thermodynamics of clays. In F. Wypych & K. G. Satyanarayana (Eds.), *Clay Surfaces: Fundamentals and Applications* (pp. 91–117). The Netherlands: Elsevier.
Jayrajsinh, S., Shankar, G., Pharm, M., Agrawal, Y. K., & Bakre, L. (2017). Montmorillonite nanoclay as a multifaceted drug-delivery carrier: A review. *Journal of Drug Delivery Science and Technology, 39*, 200–209.
Kaelble, D. H. (1970). Dispersion-polar surface tension properties of organic solids. *The Journal of Adhesion, 2*, 66–81.
Kahr, G., & Madsen, F. T. (1995). Determination of the cation exchange capacity and the surface area of bentonite, illite, and kaolinite by methylene blue adsorption. *Applied Clay Science, 9*, 327–336.
Kaufhold, S., Chryssikos, G. D., Kacandes, G., Gionis, V., Ufer, K., & Dohrmann, R. (2019). Geochemical and mineralogical characterisation of smectites from the Ventzia basin, western Macedonia, Greece. *Clay Minerals, 54*, 95–107.
Keller, W. D., Reynolds, R. C., & Inoue, A. (1986). Morphology of clay minerals in the smectite-to-illite conversion series by scanning electron microscopy. *Clays and Clay Minerals, 34*, 187–197.
Lagaly, G., & Dekany, I. (2013). *Colloid clay science*, *Pp. 243–345 in: Developments in Clay Science* (G. Lagaly and F. Bergaya, editors). Developments in Clay Science, 5, The Netherlands: Elsevier.
Lagaly, G., Ogawa, M., & Dekany, I. (2013). *Clay mineral-organic interactions* (G. Lagaly and F. Bergaya, editors). Developments in Clay Science, 5 The Netherlands: Elsevier. pp. 435–474.
Lee, S. Y., & Kim, S. J. (2002). Expansion of Smectite by Hexadecyltrimethylammonium. *Clays and Clay Minerals, 50*, 435–445.
Liang, H., Long, Z., Yang, S., & Dai, L. (2015). Organic modification of bentonite and its effect on rheological properties of paper coating. *Applied Clay Science, 104*, 106–109.
Majdan, M., Pikus, S., Gajowiak, A., Sternik, D., & Zięba, E. (2010). Uranium sorption on bentonite modified by octadecyltrimethylammonium bromide. *Journal of Hazardous Materials, 184*, 662–670.
Moslemizadeh, A., Aghdam, S. K., Shahbazi, K., Aghdam, H. K., & Alboghobeish, F. (2016). Assessment of swelling inhibitive effect of CTAB adsorption on montmorillonite in aqueous phase. *Applied Clay Science, 127–128*, 111–122.
Nones, J., Riella, H. G., Trentin, A. G., & Nones, J. (2015). Effects of bentonite on different cell types: A brief review. *Applied Clay Science, 105–106*, 225–230.
Orucoglu, E., & Haciyakupoglu, S. (2015). Bentonite modification with hexadecylpyridinium and aluminum polyoxy cations and its effectiveness in Se (IV) removal. *Journal of Environmental Management, 160*, 30–38.
Owens, D. K., & Wendt, R. C. (1969). Estimation of the surface free energy of polymers. *Journal of Applied Polymer Science, 13*, 1741–1747.
Rytwo, G., Serban, C., Nir, S., & Margulies, L. (1991). Use of methylene blue and crystal violet for determination of exchangeable cations in montmorillonite. *Clays and Clay Minerals, 39*, 551–555.
Schampera, B., Šolc, R., Tunega, D., & Dultz, S. (2016). Experimental and molecular dynamics study on anion diffusion in organically modified bentonite. *Applied Clay Science, 120*, 91–100.
Shah, L. A., Valenzuela, M. G. S., Ehsan, A. M., Díaz, F. R. V., & Khattak, N. S. (2013). Characterization of Pakistani purified bentonite suitable for possible pharmaceutical application. *Applied Clay Science, 83–84*, 50–55.
Taylor, R. L. (1985). Cation exchange in clays and mudrocks by methylene blue. *Journal of Chemical Technology and Biotechnology, 35A*, 195–207.
van Oss, C. J., Chaudhury, M. K., & Good, R. J. (1988). Interfacial Lifshitz-van der Waals and polar interactions in macroscopic systems. *Chemical Reviews, 88*, 927–941.
Veiskarami, M., Sarvi, M. N., & Mokhtari, A. R. (2016). Influence of the purity of montmorillonite on its surface modification with an alkyl-ammonium salt. *Applied Clay Science, 120*, 111–120.
Velde, B. (1992). *Introduction to Clay Minerals: Chemistry, Origins, Uses and Environmental Significance* (198 pp). London: Springer.
Yang, J. H., Lee, J. H., Ryu, H. J., Elzatahry, A. A., Alothman, Z. A., & Choy, J. H. (2016). Drug–clay nanohybrids as sustained delivery systems. *Applied Clay Science, 130*, 20–32.
Yeşilyurt, Z., Boylu, F., Çinku, K., Esenli, F., & Çelik, M. S. (2014). Simultaneous purification and modification process for organobentonite production. *Applied Clay Science, 95*, 176–181.
Yıldız, A., & Kuşcu, M. (2007). Mineralogy, chemistry and physical properties of bentonites from Başören, Kütahya, W Anatoloia, Turkey. *Clay Minerals, 42*, 399–414.
Yılmaz, N., & Yapar, S. (2004). Adsorption properties of tetradecyl- and hexadecyltrimethylammonium bentonites. *Applied Clay Science, 27*, 223–228.
Yu, W. H., Ren, Q. Q., Tong, D. S., Zhou, C. H., & Wang, H. (2014). Clean production of CTAB-montmorillonite: formation mechanism and swelling behavior in xylene. *Applied Clay Science, 97–98*, 222–234.
Zhang, J., Li, L., Xu, J., & Sun, D. (2014). Effect of cetyltrimethylammonium bromide addition on the emulsions stabilized by montmorillonite. *Colloid & Polymer Science, 292*, 441–447.
Zhou, C. H. (2011). An overview on strategies towards clay-based designer catalysts for green and sustainable catalysis. *Applied Clay Science, 53*, 87–96.

(Received 3 January 2019; revised 20 July 2019; AE: Reiner Dohrmann)